JBC Papers in Press. Published on October 9, 2015 as Manuscript M115.661249
The latest version is at http://www.jbc.org/cgi/doi/10.1074/jbc.M115.661249

The organophosphate degradation (*opd*) island borne esterase induced metabolic diversion in *E. coli* and its influence on *p*-nitrophenol degradation

Deviprasanna Chakka[+], Ramurthy Gudla[+], Ashok Kumar Madikonda[+],
Emmanuel Vijay Paul Pandeeti, Sunil Parthasarathy, Aparna Nandavaram
and
Dayananda Siddavattam*

Department of Animal Biology, School of Life Sciences, University of Hyderabad,
Hyderabad –500 046, India.

*****Running title: *Esterase induced metabolic diversion in E. coli.*

To whom correspondence should be addressed: Dayananda Siddavattam, Department of Animal Biology, School of Life Sciences, University of Hyderabad, Prof. C.R Rao Road, Gachibowli, Hyderabad, India 500 046, Tel.: +91 40 23134578; Fax: +91 40 23010120/145.
E-mail: sdsl@uohyd.ernet.in
[+]Authors contributed equally to the manuscript.

Keywords: biodegradation, ***Escherichia coli* (*E. coli*)**, **gene expression, gene knockout**, **metabolic regulation**, **microarray.**

Background: Due to the mobile nature of the *opd* island, identical *opd* and *orf306* sequences are found among soil bacteria.
Results: In *E. coli*, Orf306 suppresses glycolysis and the TCA cycle and promotes upregulation of alternate carbon catabolic operons.
Conclusion: The upregulated *hca* and *mhp* operons contribute to PNP-dependent growth of *E. coli.*
Significance: Together with *opd*, *orf306* contributes to the complete mineralization of OP residues.

ABSTRACT

In previous studies of the organophosphate degradation gene cluster we showed that expression of an open reading frame (*orf306*) present within the cluster in *E. coli* allowed growth on *p*-nitrophenol (PNP) as sole carbon source. We have now shown that expression of *orf306* in *E. coli* causes a dramatic up-regulation in genes coding for alternative carbon catabolism. The propionate, glyoxylate and methyl citrate cycle (MCC) pathway-specific enzymes are up-regulated, along with *hca* (phenyl propionate) and *mhp* (hydroxy phenyl propionate) degradation operons. These *hca* and *mhp* operons play a key role in degradation of PNP, enabling *E. coli* to grow using it as sole carbon source. Supporting growth experiments, PNP degradation products entered central metabolic pathways and got incorporated into the carbon backbone. The protein and RNA samples isolated from *E. coli* (pSDP10) cells grown in C^{14} labelled PNP indicated incorporation of C^{14} carbon suggesting Orf306-dependent assimilation of PNP in *E. coli* cells.

Bacterial phosphotriesterases (PTEs) are a group of structurally unrelated enzymes that cleave the triester linkage found in both organophosphate (OP) insecticides and OP nerve agents (1). Due to their broad substrate range and high catalytic efficiency they have been exploited for detection and decontamination of OP compounds (2). The PTEs have been classified into three main groups, i) the organophosphate hydrolases (OPHs), ii) methyl parathion hydrolases (MPHs), and iii) organophosphate acid anhydrases (OPAAs). Amongst the PTEs only the OPAAs have known physiological substrates and have been shown to be dipeptidases that cleave dipeptides with a prolyl residue at the carboxy terminus, hence are described as prolidases (3). The OP hydrolyzing activity of prolidases is considered to be an

ancillary activity due to the structural similarity of OP compounds to their usual substrates (3).

The physiological substrates for OPH and MPH enzymes are unknown. These enzymes are believed to have evolved in soil bacteria to counter the toxic effects of OP insecticide residues released into agricultural soils (4, 5). Bacterial OPH enzymes, besides showing high structural similarities with the quorum-quenching lactonases, possess weak lactonase activity (6, 7). Consequently the quorum-quenching lactonases are considered to be the possible progenitors of the bacterial OPH enzymes (7). Unlike the OPH enzymes, the MPHs have no structural similarity with quorum-quenching lactonases but instead are highly similar to ß-lactamases (8). The structurally diverse PTEs are therefore assumed to have evolved independently in response to OP residues accumulated in agricultural soils (9, 10).

The genetics of organophosphate degradation has attracted considerable attention among soil microbiologists. Both the OPH-encoding organophosphate degradation (*opd*) genes and the MPH-encoding methyl parathion degradation (*mpd*) genes have been shown to be part of mobile genetic elements (11, 12, 13). The lateral transfer of *opd* and *mpd* genes is evidenced by the existence of identical *opd* and *mpd* genes among taxonomically unrelated soil bacteria (14, 15). Even dissimilar indigenous plasmids found in bacteria collected from diverse geographical regions contained identical *opd* gene clusters (14). There are four indigenous plasmids in OP-degrading *Sphingobium fuliginis* ATCC 27551. Of these four plasmids the *opd* containing pPDL2 has been shown to be a mobilizable plasmid within which the *opd* region has unique organizational features (11). Along with an operon that contributes for protocatechuate degradation, the *opd* gene forms part of an active transposon (11). In addition to the degradation module, pPDL2 contains genes for plasmid mobility and site-specific integration, and the plasmid has been shown to integrate site-specifically at an artificially created attachment (*attB*) site (11). Based on such experimental observations the *opd* island carried on the mobilizable plasmid pPDL2 has been designated as an Integrative Mobilizable Element (IME).

A novel open reading frame (ORF), *orf306* has been identified within the *opd* island. It is found in between the *opd* gene and the truncated *tnpA* gene of a defective transposon, Tn*3* (13). A canonical catalytic triad typically seen in esterases and lipases was identified in Orf306 (16) and the esterase activity of the protein has been demonstrated using phenyl acetate as a substrate. As Orf306 shows very weak homology to the aromatic hydrolases such as TodF and CumD, we tried to evaluate its role in degradation of aromatic compounds and their meta-fission products (16, 17). More specifically since *p*-nitrophenol is the lone aromatic compound generated during the OPH/MPH-mediated hydrolytic cleavage of OP insecticides such as methyl parathion, parathion or sumithion, we attempted to find a role for Orf306 in *p*-nitrophenol degradation.

These studies showed unexpectedly that *Escherichia coli* MG1655 cells expressing Orf306 were capable of growth on *p*-nitrophenol as sole carbon source. While investigating the molecular basis for this unusual phenomenon, we observed an Orf306-dependent metabolic shift in *E. coli* (pSDP10) cells expressing Orf306. The catabolic pathways involved in hydroxy phenyl propionate (*hca*) and the phenyl propionate (*mhp*) operons are up regulated, and there is dramatic down regulation of the conventional glycolysis and TCA cycles. These novel observations offer a rationale for the presence of *orf306* within the *opd* island.

EXPERIMENTAL PROCEDURES

Strains and plasmids- The bacterial strains and plasmids used in the study are listed in Table 1 and primers used in the study are shown in Table 2. *E. coli* strains and *Sphingobium fuliginis* ATCC 27551 were grown either in LB medium or in minimal salts medium at 37 ºC and 30 ºC respectively. When necessary PNP was added to the culture medium as sole source of carbon. PNP concentration in the culture medium was determined spectrophotometrically (18). As more than 50 μM PNP is toxic to the cells, after the supplemented PNP was consumed, a fresh aliquot of PNP was added from the stock solution to keep the final concentration of PNP in the culture medium below 50 μM. Nitrite estimation in the spent medium of *E. coli* (pSDP10) was done following protocols described elsewhere (18).

The oxygen consumption in the resting cells of *E. coli* (pSDP10) was estimated using a Gilson oxygraph. Extraction and separation of the PNP metabolites in the culture medium of

MG1655 (pSDP10) was done using standard procedures (19). The metabolites were identified using Bruker Daltonics mass spectrometer systems. Data pertaining to the growth, nitrite estimation and oxygen consumption are the average values of three independent experiments. The restriction and other modifying enzymes were purchased from Fermentas, India. Biochemicals used for enzyme assays were procured from Sigma-Aldrich Pvt. Ltd, Bengaluru, India. The C^{14} *p*-nitrophenol (PNP) was obtained from American Radio Chemicals (ARC), Inc. St. Louis, USA. All DNA manipulations were done following standard procedures (20).

Growth of E.coli MG1655 (pSDP10) on C^{14}-PNP- MG 1655 (pSDP10) cells were grown to mid log phase in minimal salts media containing glucose as carbon source. The culture was then induced for 3 h by adding 0.5 *m*M IPTG. After induction the cells were harvested and thoroughly washed with minimal salts solution. The washed cells were dissolved in fresh minimal salts solution to a final OD of 0.05. Sterile PNP was added as a carbon source to a final concentration of 50 μM. Taking total counts into consideration, an aliquot of C^{14} labeled PNP was added to the culture medium to get a final count of 1000 Bq. The culture was allowed to grow until the culture reached 0.1 OD units. Once added PNP was consumed a fresh aliquot of unlabelled and labeled PNP (1000 Bq) was added to keep the concentration of added PNP at 50 μM. Protein samples were extracted from 1 ml culture and analyzed on SDS PAGE along with protein samples prepared from the cultures grown using unlabelled PNP. The gel was dried and the autoradiogram was developed following standard procedures. The total RNA isolated from the labeled and unlabeled PNP grown cultures was analyzed on an agarose gel and the autoradiogram was developed after transferring the RNA onto a nylon membrane.

Transcriptome analysis- Total RNA was isolated from *E. coli* cells using Trizol reagent (Sigma-Aldrich) following standard procedures and stored at -80 ºC in 70% v/v ethanol until further use. When required the RNA was precipitated and used for RT-PCR and qPCR experiments following standard procedures (21).

Probe design- Agilent Custom Gene Expression *E. coli* MG1655 8x15K (GT_CAT_11 - AMADID: 019439) designed by Genotypic Technology Private Limited with the probes having 45-60 mer oligonucleotides from CDS sequences downloaded from NCBI of *E. coli* MG1655. The 8x15K array comprised of 15744 features including 15208 probes and 536 Agilent controls. All the oligonucleotides were designed and synthesized *in situ* as per the standard algorithms and methodologies used by Agilent Technologies for 45-60 mer *in situ* oligonucleotide microarray. On average 3 probes were designed for 4294 coding regions and one probe for each of the 172 structural RNA sequences. It also contains 2 probes for each of the 2240 non-coding regions. For non-coding regions 2 probes were designed in both sense and antisense direction. Blast was performed against the CDS sequence databases to check the specificity of the probes. Finally, 15208 probes were designed.

Labeling and Hybridization- E. coli MG1655 (pSDP10) cells were grown to mid log phase in minimal salts medium containing glucose as sole carbon source. The culture was then induced by adding 0.5 *m*M IPTG and the total RNA was isolated from the induced culture at 0, 1.5 and 3.0 h after induction. MG1655 (pMMB206) cells grown under similar conditions served as controls. The samples were labeled using an Agilent Quick Amp Kit (Part number: 5190-0442). About 500 *n*g of total RNA was reverse transcribed using random hexamer primer tagged to T7 promoter sequence. cDNA thus obtained was converted to double stranded cDNA in the same reaction. The cDNA was then converted to cRNA in an *in vitro* transcription step using T7 RNA polymerase enzyme and Cy3 dye was added into the reaction mix. During cRNA synthesis Cy3 dye was incorporated into the newly synthesized cRNA strands. cRNA obtained was cleaned up using Qiagen RNeasy columns (Qiagen, Cat No: 74106). The concentration and amount of dye incorporated was determined using a Nanodrop. Samples that passed the QC for specific activity were taken for hybridization. 2 μg of Cy3 labeled cRNA samples were mixed and hybridized on the array using the Gene Expression Hybridization kit (Part Number 5190-0404; Agilent) in Sure hybridization Chambers (Agilent) at 65 ºC for 16 h. Hybridized slides were washed using Agilent Gene Expression wash buffers (Part No: 5188-5327). The hybridized, washed microarray slides

were then scanned at 5 micron resolution on a G2505C scanner (Agilent Technologies).

Microarray Data Analysis- Images were quantified using Agilent Feature Extraction Software. Feature extracted raw data was analyzed using Agilent GeneSpring GX software. Normalization of the data was done in GeneSpring GX using the 75th percentile shift method. Significantly up and down regulated genes (one fold and above within the samples with respect to control sample) were identified.

Quantitative Real Time PCR- Isolation of total RNA and cDNA synthesis was done as described in aforementioned sections. When multiple gene expression analysis was performed, 16s rRNA gene was taken as an internal control for the expression calibration of other genes. DNA sequences of target genes of *E. coli* were retrieved from GenBank. The Primer 3 program available online was used for primer design (http://www.ncbi.nlm.nih.gov/tools/primer-blast/). For each target gene, a primer pair capable of amplifying a DNA fragment of about 150-250bp was chosen and commercially synthesized at Sigma-Aldrich pvt. Ltd, Bengaluru, India. Quantitative PCR (qPCR) reactions were conducted in an Eppendorf qPCR machine operating with Realplex 2.2 software using 30 ng cDNA template, 0.25 μM primers and Brilliant SYBR Green reagents (Bio-Rad). Data were normalized to 16s rRNA and analyzed by absolute quantification by comparing the C_t value of the test sample to a standard curve (21).

Absolute quantification of target genes- In order to quantify the expression levels of a target gene, the amplicons of each target gene were cloned into vector pTZ57R/T (Thermo Scientific). Using these constructs as template, a 10-60 fold dilution series was made resulting in a set of standards containing 10^2-10^8 copies of the target gene. The standards and test samples were assayed in the same run. A standard curve was constructed, with the logarithm of the initial copy number of the standards plotted along the x-axis and their respective C_t values plotted along the y-axis. Finally, the copy number of the target gene in the test sample was obtained by interpolating its C_t value against the standard curve.

E. coli knockouts- Phage P1 particles were prepared by infecting appropriate mutant strains of *E. coli* K-12 BW1153. These P1 particles were then incubated with an overnight culture (2 ml) of MG1655 cells. After adding 5 *m*M $CaCl_2$ the contents were incubated at 37 ^{o}C to facilitate absorption of P1 particles. The unabsorbed phage particles were removed by centrifugation and the cell pellet was re-suspended in 5 ml of LB broth containing 5 *m*M sodium citrate. The culture was then incubated for a further period of 45 min at 37 °C with mild shaking. After incubation the cells were harvested and plated on LB pate containing 5 *m*M sodium citrate and 30 μg/ml of kanamycin. The kanamycin resistant colonies were screened to confirm mutation by performing PCR amplification with gene-specific primers. MG1655 cells having deletions in *hcaR*, *mhpA*, *mhpR*, *paaA* and *maoA* were transformed with pSDP10 and were tested for their ability to grow using PNP as sole source of carbon.

Proteomics- MG1655 cultures carrying the Orf306 expression plasmid pSDP10 or the control vector pMMB206 were grown in minimal medium containing glucose as sole source of carbon. When the cultures reached mid-log phase they were induced for one and half hours with IPTG (0.5 *m*M). The total soluble proteins extracted from these cultures were subjected to IEF and second dimension electrophoresis (22). The proteome maps generated for both strains were compared and the protein spots that were either up-regulated or down-regulated were identified by image analysis using ImageMaster 2D platinum software (GE Healthcare). The differentially and differently expressed proteins were identified by MALDI TOF/TOF Autoflex (Bruker Daltonics) and the MASCOT search engine (http://www.matrixscience.com) against Swiss-port (http://www.expasy.ch/sport) and NCBI (http://www.ncbi.nlm.nih.gov) following procedure optimized in our laboratory (22).

Reciprocal pull-down assays- The *orf306* and *opd* genes were cloned in compatible plasmids to code for Orf306 and OPH^{6xHis}. *E. coli* BL21 carrying either pSM5 or pSM5 and pSDP5 were induced following standard procedures. Clear lysates were prepared and incubated with 100 μl of MagneHis^{TM} (Promega) beads for 4 h. After incubation, the beads were collected and were washed thoroughly with buffer containing 50

*m*M imidazole. Finally, protein bound to the beads were eluted by adding buffer containing 500 *m*M imidazole. The eluted sample was mixed with 2x Laemmli buffer and analysed on SDS-PAGE. Similarly OPH^{6xHis} (pSM5) and $Orf306^{GST}$ (pSDP4) were expressed in *E. coli* BL21. The protein lysate was passed through a glutathione sepharose column (GE healthcare) and after through washing, eluted using buffer containing glutathione. The samples were analysed on SDS-PAGE and western blot was performed by probing with either anti-OPH antibodies or with anti-GST antibodies. The cell lysates prepared from BL21 (pSM5+pGEX-4T1) cells served as controls.

Promoter assays- Both quantitative and qualitative assays were performed to assess promoter activity of *hcaR*, *mhpR* and *mhpA* genes. Initially the promoters of these genes were amplified using primers sets shown in Table 2 and cloned in promoter test vector pMMP220. The respective promoter *lacZ* fusions were transformed into *lacZ* negative strains of *E. coli* MG1655 and used for performing both quantitative and qualitative promoter assays. While performing qualitative assays the minimal medium plates were prepared by supplementing M9 medium with X-gal (40 μg/ml) and propionate (20 *m*M) as sole source of carbon. *E. coli* MG1655, as well as cells containing vector p P220 and promoter-lacZ fusions were plated on propionate plates before incubating them for 72 hours at 37 °C. Similar cultures grown on M9 medium containing glucose as source of carbon served as controls. The *E coli* MG1655 cells with promoter-*lacZ* fusions and the vector were grown to mid-log phase in propionate medium containing tetracycline (10μg/ml). Cells from 1ml culture were harvested and promoter activity was quantified by performing β-galactosidase activity (23).

Cloning and expression of hca operon- The HcaEFBCD ORFs were amplified from the *hca* operon as an NdeI/SalI fragment and cloned in pET23b to generate expression plasmid pNS1. Plasmid pNS1 codes for $HcaEFBCD^{6xHis}$. Plasmids pAS1 and pNS1 were transformed into BL21 and induced following standard procedures (20). Metal affinity chromatography using Ni-column was performed to purify $HcaEFBCD^{6xHis}$ complex.

RESULTS

PNP metabolism in E. coli (pSDP10)- E. coli has not previously been observed to use PNP as a sole source of carbon (24). We therefore conducted a series of *in vitro* and *in vivo* studies to gain better insights into this unusual process. In these studies we used plasmid pSDP10 which expresses *orf306* under the control of an inducible *tac* promoter.

To assess whether PNP is a direct substrate of Orf306 we performed *in vitro* studies by incubating purified Orf306 with PNP. The concentration of PNP in the reaction mixture remained unaltered even after prolonged incubation (12 h) suggesting that PNP is not a direct substrate of Orf306. However, when assayed for esterase activity, Orf306 was active and showed a specific activity of 0. 236 *n*moles/mg/minute. Although, purified Orf306 failed to degrade PNP, when the growth properties of *E. coli* MG1655 (pSDP10) cells were examined the influence of Orf306 on PNP catabolism was apparent (Fig. 1*A*). If PNP supports Orf306-dependent growth its degradation products should gain entry into the carbon backbone of MG1655 (pSDP10) cells. Providing solid evidence on Orf306-dependent PNP assimilation in MG1655 (pSDP10) cells the C^{14} carbon associated with C^{14}-labelled PNP became incorporated into proteins and RNA molecules (Fig. 1, *B* and *C*). This is direct evidence to show that the catabolic intermediates generated from PNP gain entry into central metabolic pathways and generate precursor molecules necessary for synthesis of macromolecules like proteins and RNA.

Resting cells of MG1655 (pSDP10) consumed three moles of oxygen for every one mole of *p*-nitrophenol degraded (data not shown) indicating involvement of Orf306 induced oxygenases in the degradation of PNP. The cells also released nitrite in a stoichiometric relationship to PNP depletion, suggesting hydroxylation of PNP at the *para* position (Fig. 1*D*). Furthermore, PNP metabolites such as nitrocatechol (4.5) and benzenetriol (8.3) were also detected in the culture medium (Fig. 1*E* and *F*). Detection of nitrocatechol and benzenetriol indicated involvement of typical hydroxylation steps during PNP degradation in MG1655 (pSDP10) cells (19, 24). Since, Orf306 showed no direct activity on PNP it seemed possible that its influence on PNP catabolism might be through induction of novel proteins or pathways.

PP and HPP pathways contribute to PNP catabolism- In order to investigate the catabolome involved in PNP degradation we performed 2D electrophoresis of the proteome extracted from MG1655 (pSDP10) cells. When compared with a similar map generated from a control strain, MG1655 (pMMB206), that did not express Orf306, the proteome map of these cells revealed up-regulation of several protein spots. Most notable among them were HcaR (Fig. 2*B*), the transcriptional activator of the phenyl propionate degradation operon (*hca*), and 3-hydroxy phenyl propionate oxygenase (MhpA) (Fig. 2*B*). These two proteins play a key role in phenyl propionate (PP) and hydroxy phenyl propionate (HPP) catabolism (24). Up-regulation of the PP and HPP pathway enzymes suggests a possible role for the PP and HPP pathway-specific oxygenases in the oxidation of PNP in MG1655 (pSDP10) cells.

The *pp* and *hpp* operons are normally tightly regulated in MG1655 and are only induced in presence of their cognate substrates (24, 25, 26). However, the presence of Orf306 induced expression of these two tightly regulated operons in MG1655 (pSDP10) cells grown in minimal medium containing glucose as the only source of carbon. Anticipating a major shift in carbon catabolism in MG1655 (pSDP10) cells, we carried out genome-wide expression profiling for MG1655 cells with and without *orf306*. Both strains were grown in glucose-containing minimal medium with neither PNP nor any other aromatic compound to serve as an alternative carbon source. Total RNA was extracted from these induced cultures, 0, 1.5 and 3.0 h after induction and used to synthesise labelled cDNA. Analysis of the global transcription expression profiles revealed upregulation of the *hca* and *mhp* operons in MG1655 (pSDP10) cells (Fig. 2 *C*). Furthermore expression of other two operons, *paa* and *mao*, involved in aromatic compound utilization remained unaltered, suggesting possible involvement of the *hca* and *mhp* operons in PNP degradation (Fig. 2*A*). To test this hypothesis, MG1655 null mutants were generated by deleting key genes in each of the four operons involved in aromatic compound degradation (Fig. 2*E* and *G*). These mutants were then independently tested for growth on minimal medium containing PNP. PNP-dependent growth was not observed in *hca* and *mhp* null mutants of MG1655 (pSDP10) (Fig. 2*D*). However, PNP-dependent growth was seen in MG1655 (pSDP10) *paaA* and *maoA* negative mutants, providing conclusive evidence for the involvement of the *hca* and *mhp* operons in Orf306-dependent degradation of PNP (Fig. 2*F*).

Upregulation of the alternate carbon utilization pathways in MG1655 (pSDP10)-The aforementioned results implicated Orf306-dependent induction of the *hca* and *mhp* operons and their involvement in PNP degradation. However, when the heat map generated from microarray data was examined, it indicated major alterations in the expression profile of other genes involved in carbon catabolism. In particular, a significant decrease was observed in the transcription of genes coding for glycolysis and TCA cycle enzymes. The decrease in the expression pattern of these pathway-specific genes started soon after induction of Orf306 and the repressive trend increased up to 3 h after induction (Fig. 3). To gain supportive evidence for the microarray data, qPCR experiments were performed to quantify expression of certain key glycolysis and TCA cycle-specific genes. As expected there was more than a 3-fold reduction in the expression of phosphofructokinase (*pfkA*), enolase (*eno*) and aconitase (*acnA*) genes consistent with repression of glycolysis and the TCA cycle in MG1655 (pSDP10) cells (Fig. 3).

Interestingly the heat map also revealed a significant increase in the expression of genes coding for alternative carbon catabolic pathways. The genes coding for the propionate catabolic pathway, the methyl citrate cycle (MCC), and glyoxylate pathways showed significant induction in the presence of Orf306. The qPCR performed for *glcC* and *glcB* supported the microarray findings and is consistent with up-regulation of the glyoxylate pathway (Fig. 3). A similar trend was seen in the proteomics data. The 2D gels clearly indicated Orf306-dependent up-regulation of methyl isocitratelyase (PrpB) and the transcription factor GlcC in MG1655 (pSDP10) cells (Fig. 3). The transcription activator GlcC activates the *glc* operon and contributes to induction of glycolate oxidase (GlcD, E, F) and malate synthase G (GlcB), providing conclusive evidence for the up-regulation of the glyoxylate pathway. Taken together with up-regulation of PP and HPP-specific enzymes, this shift in carbon catabolic pathways is very significant because the end products generated from PNP degradation, such as succinyl-CoA and acetyl-CoA, gain direct entry into the TCA and glyoxylate pathways.

Orf306 contains a lipase/esterase domain and its esterase activity is apparent when assayed following standard procedures (27). *E. coli* cells have been shown to use endogenous fatty acids as source of carbon in an FadD-dependent manner (28). In such cells, as seen in present study, glyoxalate pathway enzymes are upregulated (29). One possible hypothesis was that the lipase activity of Orf306 in *E. coli* could generate odd chain fatty acids which when oxidised to propanoyl-CoA could lead to induction of the propionate catabolic operon. If this hypothesis is correct the propionate should also serve as a signalling molecular for induction of the *hca* and *mhp* operons that are shown to play a key role in PNP degradation. The *hpp* and *mhp* operons are positively regulated by transcription factors HcaR and MhpR (26). To examine the link between propionate generation and the induction of the *pp* and *hpp* operons, we assayed promoter activity of *hcaR*, *mhpR* and *mhpA* genes in the presence of propionate. Interestingly, propionate induced transcription of both the *hcaR* and *mhpR* genes. However, the propionate-dependent activity of the *hcaR* promoter was five-fold higher than that of the *mhpR* promoter (Fig. 4*A* and *B*). Nonetheless, when grown in glucose, such induction of the *hcaR* and *mhpR* genes was seen only in IPTG-induced cells of MG1165 (pDS10) expressing *orf306* (Fig. 4*F*) and not in an *orf306* negative background (Fig. 4*C* and *D*). The HcaR concentration in *E. coli* is negligible in early and mid log phase cultures. Its concentration dramatically increases during stationary phase in an RpoS-independent manner (25). In order to rule out the possibility of RpoS involvement in *hcaR* induction we assayed promoter activities of *hcaR* and *mhpR* in early log phase cultures (25). The data obtained through quantitative and qualitative assays clearly indicated propionate-dependent induction of *hcaR* and *mhpR*, suggesting that the propionate generated due to the esterase/lipase activity of Orf306 is responsible for the induction of *hcaR* and *mhpR*.

Genetic evidences gathered in this study clearly suggested requirement of both *hca* and *mhpA* operons for degradation of PNP (Fig. 2). Since propionate induces expression of HcaR, the transcriptional activators of the *hca* operon, we designed further experiments to gain biochemical evidence between *hca* operon and PNP degradation. The products of the *hca* operon convert phenyl propionate (PP) to dihydroxy phenyl propionate (DHPP). The HcaEFCD complex, otherwise known as PP dioxygenase, converts PP to PP-dihydrodiol (24, 25). PP-dihydrodiol dehydrogenase, the product of *hcaB*, converts PP-dihydrodiol to DHPP. Hydroxylation is the first step in biodegradation of PNP. Assuming that the *hca* operon has role in hydroxylation of PNP, we have attempted to conduct *in vitro* studies using purified HcaEFBCD complex. Our attempts to obtain pure HcaEFBCD^{6xHis} complex from the induced BL21 (pNS1) cells gave no positive results. The cell lysate when analyzed on SDS-PAGE showed existence of all other subunits except HcaC and HcaD^{6xHis} (Supplementary Fig. 1). In order to gain further insights into these unexpected results, the gel was used to perform immunoblot using anti-His antibodies, to detect HcaD^{6xHis}. Surprisingly we have obtained signal at a position far below the predicted mass (43Kda) of HcaD^{6xHis}, suggesting degradation of HcaD^{6xHis} in BL21 (pNS1) cells. Changes in induced conditions, IPTG concentration gave no positive results. In the absence of HcaD^{6xHis} it was not possible to obtain pure HcaEFBCD^{6xHis} complex. Therefore we failed to gain biochemical support for our genetic evidence that suggests involvement of *hca* operon in degradation of PNP.

In the sequence of plasmid pPDL2 we have noticed a *lig* operon coding for a 4, 5 dioxygenase along with an ORF that codes for a LysR-type transcription factor. These two genes are located in the upstream region along with the *opd* gene and *orf306* and all of them are part of the *opd* island (11). It is not known if there is a link between Orf306 and expression of this dioxygenase and transcription factor. Existence all these genes as part of *opd* island and considerable sequence homology between HcaR and the *opd* island-borne LysR homologue may be significant with respect to the mechanism underlying esterase-dependent activation of *hcaR*.

Having established the influence of Orf306 on *p*-nitrophenol catabolism in *E. coli*, and observed a related Orf306-dependent shift in carbon metabolism, we conducted further experiments to examine the expression and sub-cellular localization of Orf306 in *S. fuliginis* ATCC. Membrane-associated OPH, the product of *opd* gene, initiates degradation by cleaving the triester linkage found in organophosphates. The genetically linked *opd* and *orf306* are flanked by mobile elements IS*21* and Tn*3* to facilitate their lateral transfer (13) and hence we

were interested in their potential co-localisation within the cell.

The Orf306-specific signal was observed in protein extracts prepared form *S. fuliginis* ATCC 27551 and, on closer examination of the western blot, the protein appeared to be a doublet. The two forms of Orf306 show an approximately 2 Kda size difference and suggest the possibility of posttranslational modification of Orf306 when expressed in *S. fuliginis* ATCC 27551. Studies of the sub-cellular localization of these two forms of Orf306 showed the modified form to be exclusively found in the membrane whilst the unmodified version was only seen in cytoplasm (Fig. 5 A and B). Hence both OPH and the presumptively modified form of Orf306 are membrane associated, and assuming that this may have functional relevance we conducted experiments to ascertain if there are any physical interactions between these two proteins. The reciprocal pull-down experiments were performed by co-expressing these two proteins in *E. coli* with two different affinity tags. The pull down experiments gave a clear indication of possible interactions between these two proteins (Fig. 5C, D, E and F). If these interactions are seen together with Orf306-induced metabolic reprogramming in *E. coli* it points towards existence of an OPH-Orf306-mediated signalling mechanism in *S. fuliginis* ATCC 27551. The existence of *hcaR* and *hcaA* functional homologues, *lysR* and *lig*, as part of the *opd* island and Orf306-dependant induction of these genes in *E. coli* adds strength to this proposition (11).

DISCUSSION

Organophosphates were introduced as pest control agents to replace the most persistent organochloride insecticides and they are now the most predominant insecticides used in world agriculture. Although they are less persistent in the environment, their degradation products such as PNP are highly persistent and toxic to soil microbes. Therefore metabolic diversion towards use of compounds like PNP as a source of carbon, as we observed when Orf306 was expressed in *E. coli*, is advantageous and can contribute to organismal fitness. We set out to establish a link between Orf306 and the induction of alternate carbon catabolic pathways and this study led us to reveal novel regulatory mechanisms hitherto unknown in *E. coli*. Interestingly, our investigations have revealed propionate-dependent induction of the transcription factors, HcaR and MhpR. Considerable attempts have been made to understand regulation of *hcaR* and *mhpR* expression (25) and none of them have shown propionate as an inducer of the *hcaR* and *mhpR* genes. Though the mechanistic details are still unclear, our studies clearly demonstrate the existence of a positive influence of propionate on the expression of these two genes. Apparently these transcription factors contribute to the upregulation of the *hca* (phenyl propionate) and *mhp* (hydroxy phenyl propionate) degradation operons (24). The results presented in this study clearly demonstrate involvement of these two operons in degradation of *p*-nitrophenol (PNP). If propionate-dependent induction of the *hca* and *mhp* operons is considered together with the esterase/lipase activity of Orf306, the endogenous propionate generated in *E. coli* (pSDP10) cells appears to be the precise link between Orf306 and the induction of these two operons. The existence of a PNP monoxygenase activity in HcaEFCD-expressing *E. coli* cells provides conclusive evidence to show a link between ORf306 expression and utilization of PNP as carbon source by *E. coli* (pSDP10) cells.

In the *opd* island on plasmid pPDL2, *orf306*, which codes for the esterase, is located between the *opd* gene and the *tnpA* gene which codes for a truncated transposase of a defective transposon Tn*3*. There is no detectable terminator motif between *orf306* and *tnpA* which originally led us to deduce that these two genes are co-transcriptional. However, RT-PCR and promoter assays have clearly shown that *orf306* is an independent transcriptional unit (data not shown). The dissimilar *opd* plasmids pCMS1 and pPDL2 are mobilizable in nature and possess absolute sequence identity in the DNA region containing the *opd* gene, the IS element IS*21* and *orf306*. However in pCMS1 the sequence coding *orf306* is extended to give an ORF coding for a 345 amino acid carboxyesterase which appears to form an operon along with an ORF coding for amidase (30). In pPDL2 insertion of Tn*3* in *orf345* appears to have created *orf306* and generated the genetic organization seen in this plasmid. That organization which resembles a complex transposon suggests possible reasons for the existence of identical *opd* regions in taxonomically diverse microbes (30).

Orf306-dependent PNP catabolism has significant advantage for soil microbes. PNP is

the lone aromatic compound generated during PTE-mediated hydrolysis of OP insecticides. Bacterial strains having exclusive PNP degradation pathways are known both in Gram positive and Gram negative soil bacteria (18, 19). However most of them fail to show PTE activity. Unless PNP degradation capability is laterally transferred along with PTE coding sequences its contribution to the total elimination of OP residues is compromised. The existence of *orf306* as part of a PTE-coding integrative mobilizable element (IME) is therefore advantageous to soil microbes as it enables the recipient cells to use OP residues as source of carbon.

Acknowledgements: DPC, RG and AM thank ICMR and CSIR for providing research fellowships. Research support given by CSIR, DST and DBT to DS laboratory is highly acknowledged. Dept. of Animal Biology is a DST-FIST supported Department. The School of Life Sciences, University of Hyderabad is supported by DBT-CREBB and UGC-CAS. We thank Dr. M. J. Merrick for critical reading of the manuscript and Dr. Manjula Reddy for useful suggestions and providing *E. coli* mutants. Genotypic technology Pvt. Ltd. Bengaluru is acknowledged for their help in transcriptome data analysis.

Conflict of interest: The authors declare that they have no conflicts of interest with the contents of this article.

Author contributions: DPC, RG, AM and AN conducted the experiments. EVP and SP analysed the microarray data. DS designed the experiments and prepared the manuscript.

REFERENCES

1. Singh, B. K., and Walker, A. (2006) Microbial degradation of organophosphorus compounds. *FEMS microbiology reviews* **30**, 428-471.
2. Singh, B. K. (2009) Organophosphorus-degrading bacteria: ecology and industrial applications. *Nature reviews. Microbiology* **7**, 156-164.
3. Stepankova, A., Duskova, J., Skalova, T., Hasek, J., Koval, T., Ostergaard, L. H., and Dohnalek, J. (2013) Organophosphorus acid anhydrolase from Alteromonas macleodii: structural study and functional relationship to prolidases. *Acta crystallographica. Section F, Structural biology and crystallization communications* **69**, 346-354.
4. Bar-Rogovsky, H., Hugenmatter, A., and Tawfik, D. S. (2013) The evolutionary origins of detoxifying enzymes: the mammalian serum paraoxonases (PONs) relate to bacterial homoserine lactonases. *The Journal of biological chemistry* **288**, 23914-23927.
5. Roodveldt, C., and Tawfik, D. S. (2005) Shared promiscuous activities and evolutionary features in various members of the amidohydrolase superfamily. *Biochemistry* **44**, 12728-12736.
6. Afriat, L., Roodveldt, C., Manco, G., and Tawfik, D. S. (2006) The latent promiscuity of newly identified microbial lactonases is linked to a recently diverged phosphotriesterase. *Biochemistry* **45**, 13677-13686.
7. Merone, L., Mandrich, L., Rossi, M., and Manco, G. (2005) A thermostable phosphotriesterase from the archaeon Sulfolobus solfataricus: cloning, overexpression and properties. *Extremophiles : life under extreme conditions* **9**, 297-305.
8. Garau, G., Di Guilmi, A. M., and Hall, B. G. (2005) Structure-based phylogeny of the metallo-beta-lactamases. *Antimicrobial agents and chemotherapy* **49**, 2778-2784.
9. Afriat-Jurnou, L., Jackson, C. J., and Tawfik, D. S. (2012) Reconstructing a missing link in the evolution of a recently diverged phosphotriesterase by active-site loop remodeling. *Biochemistry* **51**, 6047-6055.
10. Copley, S. D. (2009) Evolution of efficient pathways for degradation of anthropogenic chemicals. *Nature chemical biology* **5**, 559-566.
11. Pandeeti, E. V., Longkumer, T., Chakka, D., Muthyala, V. R., Parthasarathy, S., Madugundu, A. K., Ghanta, S., Medipally, S. R., Pantula, S. C., Yekkala, H., and Siddavattam, D. (2012)

Multiple mechanisms contribute to lateral transfer of an organophosphate degradation (opd) island in Sphingobium fuliginis ATCC 27551. *G3* **2**, 1541-1554.
12. Wei, M., Zhang, J. J., Liu, H., Wang, S. J., Fu, H., and Zhou, N. Y. (2009) A transposable class I composite transposon carrying mph (methyl parathion hydrolase) from Pseudomonas sp. strain WBC-3. *FEMS microbiology letters* **292**, 85-91.
13. Siddavattam, D., Khajamohiddin, S., Manavathi, B., Pakala, S. B., and Merrick, M. (2003) Transposon-like organization of the plasmid-borne organophosphate degradation (opd) gene cluster found in Flavobacterium sp. *Applied and environmental microbiology* **69**, 2533-2539.
14. Mulbry, W. W., Kearney, P. C., Nelson, J. O., and Karns, J. S. (1987) Physical comparison of parathion hydrolase plasmids from Pseudomonas diminuta and Flavobacterium sp. *Plasmid* **18**, 173-177.
15. Zhang, R., Cui, Z., Zhang, X., Jiang, J., Gu, J. D., and Li, S. (2006) Cloning of the organophosphorus pesticide hydrolase gene clusters of seven degradative bacteria isolated from a methyl parathion contaminated site and evidence of their horizontal gene transfer. *Biodegradation* **17**, 465-472.
16. Khajamohiddin, S., Babu, P. S., Chakka, D., Merrick, M., Bhaduri, A., Sowdhamini, R., and Siddavattam, D. (2006) A novel meta-cleavage product hydrolase from Flavobacterium sp. ATCC27551. *Biochemical and biophysical research communications* **351**, 675-681.
17. Khajamohiddin, S., Repalle, E. R., Pinjari, A. B., Merrick, M., and Siddavattam, D. (2008) Biodegradation of aromatic compounds: an overview of meta-fission product hydrolases. *Critical reviews in microbiology* **34**, 13-31.
18. Kadiyala, V., and Spain, J. C. (1998) A two-component monooxygenase catalyzes both the hydroxylation of p-nitrophenol and the oxidative release of nitrite from 4-nitrocatechol in Bacillus sphaericus JS905. *Applied and environmental microbiology* **64**, 2479-2484.
19. Pakala, S. B., Gorla, P., Pinjari, A. B., Krovidi, R. K., Baru, R., Yanamandra, M., Merrick, M., and Siddavattam, D. (2007) Biodegradation of methyl parathion and p-nitrophenol: evidence for the presence of a p-nitrophenol 2-hydroxylase in a Gram-negative Serratia sp. strain DS001. *Applied microbiology and biotechnology* **73**, 1452-1462.
20. Sambrook, J., and Russell David, W. (1989) *Molecular cloning: a laboratory manual. Vol. 3*, Cold spring harbor laboratory press.
21. Longkumer, T., Parthasarathy, S., Vemuri, S. G., and Siddavattam, D. (2014) OxyR-dependent expression of a novel glutathione S-transferase (Abgst01) gene in Acinetobacter baumannii DS002 and its role in biotransformation of organophosphate insecticides. *Microbiology* **160**, 102-112.
22. Pandeeti, E. V., Chinnaboina, M. R., and Siddavattam, D. (2009) Benzoate-mediated changes on expression profile of soluble proteins in Serratia sp. DS001. *Letters in applied microbiology* **48**, 566-571.
23. Miller, J. H. (1972) Experiments in molecular genetics. *CSHL Press*.
24. Diaz, E., Ferrandez, A., Prieto, M. A., and Garcia, J. L. (2001) Biodegradation of aromatic compounds by Escherichia coli. *Microbiology and molecular biology reviews : MMBR* **65**, 523-569.
25. Turlin, E., Perrotte-piquemal, M., Danchin, A., and Biville, F. (2001) Regulation of the early steps of 3-phenylpropionate catabolism in Escherichia coli. *Journal of molecular microbiology and biotechnology* **3**, 127-133.
26. Manso, I., Torres, B., Andreu, J. M., Menendez, M., Rivas, G., Alfonso, C., Diaz, E., Garcia, J. L., and Galan, B. (2009) 3-Hydroxyphenylpropionate and phenylpropionate are synergistic activators of the MhpR transcriptional regulator from Escherichia coli. *The Journal of biological chemistry* **284**, 21218-21228.
27. Huggins, C., and Lapides, C (1947) Chromogenic substrates: IV. Acyl esterases of *p*-Nitrophenol as substrates for the colorimetric determination of esterase. *J. Biol. Chem.***170**, 467-482.
28. Pech-Canul, A., Nogales, J., Miranda-Molina, A., Alvarez, L., Geiger, O., Soto, M. J., and Lopez-Lara, I. M. (2011) FadD is required for utilization of endogenous fatty acids released from membrane lipids. *Journal of bacteriology* **193**, 6295-6304.

29. Walsh, K., and Koshland, D. E. Jr (1984) Determination of flux through a branch point of two metabolic cycles. The tricarboxylic acid cycle and the glyoxylate shunt. *J. Biol. Chem.***259,** 9646-9654.
30. Pandeeti, E. V., Chakka, D., Pandey, J. P., and Siddavattam, D. (2011) Indigenous organophosphate-degrading (opd) plasmid pCMS1 of Brevundimonasdiminuta is self-transmissible and plays a key role in horizontal mobility of the opd gene. *Plasmid* **65**, 226-231.
31. Blattner, F. R., Plunkett, G., 3rd, Bloch, C. A., Perna, N. T., Burland, V., Riley, M., Collado-Vides, J., Glasner, J. D., Rode, C. K., Mayhew, G. F., Gregor, J., Davis, N. W., Kirkpatrick, H. A., Goeden, M. A., Rose, D. J., Mau, B., and Shao, Y. (1997) The complete genome sequence of Escherichia coli K-12. *Science* **277**, 1453-1462.
32. Kawahara K, Tanaka A, Yoon J ,and Yokota A (2010) Reclassification of a parathione-degrading *Flavobacterium* sp. ATCC 27551 as *Sphingobium fuliginis* J. Gen. Appl. Microbiol.,**56** : 249-255.
33. Morales, V. M., Backman, A., and Bagdasarian, M. (1991) A series of wide-host-range low-copy-number vectors that allow direct screening for recombinants. Gene 97, 39-47.
34. Spaink, H. P., Okker, R. J., Wijffelman, C. A., Pees, E., and Lugtenberg, B. J. (1987) Promoters in the nodulation region of the Rhizobium leguminosarum Sym plasmid pRL1JI. *Plant molecular biology* **9**, 27-39.

FOOTNOTES

[1]To whom correspondence should be addressed: Dayananda Siddavattam, Department of Animal Biology, School of Life Sciences, University of Hyderabad, Prof. C.R Rao Road, Gachibowli, Hyderabad, India 500 046, Tel.: +91 40 23134578; Fax: +91 40 23010120/145; E-mail: sdsl@uohyd.ernet.in

[2]The abbreviations used are: PNP, para-nitrophenol; OP, Organophosphate; *orf306*, open reading frame 306; OPH, Organophosphorous hydrolase.

FIGURE LEGENDS

FIGURE 1. *PNP supported growth of E. coli MG1655 (pSDP10)*- Panel A indicates growth of MG1655 (pSDP10), MG1655(pMMB206) and MG1655 cells in PNP-containing minimal medium. Closed (growth) and open (PNP) circles represent growth and PNP concentration in culture medium containing MG1655 (pSDP10). Similar parameters are indicated with closed (growth) and open (PNP) squares for MG1655 (pMMB206) and closed (growth) and open (PNP) rhombus for MG1655 cultures. Proteins extracted from MG1655 (pSDP10) cells grown in presence of normal and C^{14}-labeled PNP were analysed on SDS-PAGE and incorporation of C^{14} into proteins is shown in corresponding autoradiogram (Panel B). RNA extracted from similarly grown cultures and the corresponding autoradiogram is shown in Panel C. The intense sharp signal shown by the arrow indicates incorporation C^{14} into 5s rRNA. Panel D indicates decrease in concentration of PNP and concomitant release of stoichiometric amounts of nitrite in resting cells of *E. coli* (pSDP10). HPLC profile showing time dependent decrease of PNP in culture medium and appearance of nitrocatechol (4.5 mins) and benzenetriol (8.3 mins) are shown in panel E and F.

FIGURE 2. *The Orf306-dependent induction of the* hca *and* mhp *operons*- Panel A, heat map showing expression of the *hca* and *mhp* operons at 0, 1.5 and 3.0 h after induction of *orf306*. The portion of the 2-D gel showing Orf306-specific induction of HcaR and MhpA proteins is shown in panel B. The quantification (qPCR) of *mhpA, mhpR, hcaE* and *hcaR* specific transcripts under similar growth conditions are shown in panel B. Growth of the MG1655 (pDS10) (●) and *hcaE* (■), *mhpA* (▲), *mhpR* (◆) mutants in PNP-containing minimal medium is shown in panel D. Panel E represents agarose gel pictures indicating deletion of *hcaE*, *mhpA* and *mhpR* genes. The PNP-dependent growth of MG1655 (pDS10) (●), *paaA* (■), *maoA* (▲) mutants (panel F) and agarose gel showing the deletion of the *paaA* and *maoA* genes (panel G) are shown.

FIGURE 3. *Orf306-induced metabolic diversion in MG1655 (pSDP10)*- Heat maps represent differential expression of genes encoding glycolysis, glyoxylate and TCA cycle enzymes at 0, 1.5, 3.0 hrs. The green arrows represent down-regulated pathways. The up-regulated pathways are shown in

red arrows. Up-regulation of phenyl propionate pathway and down-regulation of glycolysis are shown with dotted green and red arrows respectively. Quantitative PCR results showing either Orf306-dependent decrease (*pfkA, eno* and *acnA)* or increase (*glcB, glcC* and *prpB)* in the quantity of specific mRNA concentration are inserted at places showing corresponding enzyme reactions. The 2-D gel portions indicate Orf306-dependent induction of MhpA, HcaR, GlcC, PrpB and SdhA.

FIGURE 4. *Propionate dependent induction of* hcaR *and* mhpR *genes*- The *lacZ* negative strains of MG1655 containing promoter test vector pMMP220, *hcaR, mhpR* and *mhpA lacZ* fusions are grown either in propionate+X-gal (A) or Glucose+X-gal plate (B). The quantification of promoter activity for propionate- and glucose-grown cultures are shown in panels C and D respectively. The Orf306-dependent induction of the *hcaR*, *mhpR* and *mhpA* genes in MG1655 (pSDP10) cells are shown in panel E and F respectively.

FIGURE 5. *Expression and subcellular localization of Orf306 in Sphingobium fuliginis ATCC 27551*- The proteins extracted from whole cells (W), membrane (M) and cytoplasm (C) are analysed on SDS-PAGE (Panel A). The corresponding western blot developed using Orf306-specific antibodies are shown in panel B. Arrows indicate existence of Orf306 in two different forms. The asterisk (*) indicates the exclusive presence of post translationally modified Orf306 in the membrane fraction. Reciprocal pulldown assays performed to show OPH and Orf306 interactions are shown in panels C to F. Panel C indicates proteins extracted from BL21 (pSM5) and BL21 (pSM5+pSDP5) loaded in lane 1 and 2. The corresponding pulldown samples are loaded in lanes 3 and 4. Co-elution of Orf306 along with OPH^{6xHis} is shown with an arrow (lane 4). Panel D, lane 1 and 3 represent protein extracts prepared either from BL21 (pSM5+pSDP4) or BL21 (pGEX4T1+pSM5) as input. Lane 3 and 4 represent proteins in pull-down samples. The western blots developed with either OPH-specific antibodies or with GST-specific antibodies are shown in panels E and F respectively.

TABLE 1

Strain	Genotype or Phenotype	Reference or Source
E.coli DH5α	Cloning Strain	Promega
E. coli BL21 (DE3)	*fhuA2 [lon] ompT gal (λ DE3) [dcm] ΔhsdS λ DE3 = λ sBamHIo ΔEcoRI-B int::(lacI::PlacUV5::T7 gene1) i21 Δnin5*	NEB
E. coli K-12 MG1655	F- lambda- *ilvG- rfb*-50 *rph*-1	31
Sphingobium fuliginis ATCC 27551	Wild type strain OPH^{+}, Sm^{r}, Pm^{r}	32
E. coli K-12 MG1655 (Δ***hcaE)***	F-, *λ*-, *rph-1*, Km^{r}, Null mutant of *hcaR*	This study
E. coli K-12 MG1655 (Δ***mhpA)***	F-, *λ*-, *rph-1*, Km^{r}, Null mutant of *mhpA*	This study
E. coli K-12 MG1655 (Δ***mhpR)***	F-, *λ*-, *rph-1*, Km^{r}, Null mutant of ***mhpR***	This study
E. coli K-12 MG1655 (Δ***paaA)***	F-, *λ*-, *rph-1*, Km^{r}, Null mutant of ***paaA***	This study
E. coli K-12 MG1655 (Δ***maoA)***	F-, *λ*-, *rph-1*, Km^{r}, Null mutant of ***maoA***	This study
Plasmid Name	**Description**	**Reference**
pMMB206	A low copy number broad host range expression vector, Cm^{r}	33
pMP220	Promoter test vector, Tc^{r}	34
pET23b	T7 Expression System, Amp^{r}	Novagen
pET15b	T7 expression system, Amp^{r}	Novagen
pGEX-4T1	*tac* promoter based expression system, Amp^{r}	GE Healthcare
pSDP10	*orf306* cloned as *Bgl*II fragment under the control of the inducible *tac* promoter of pMMB206 to express $Orf306^{N6xHis}$, Cm^{r}	This study
pSDP4	*orf306* cloned as a BamHI fragment in pGEX4T1. Codes for $Orf306^{NGST}$, Amp^{r}	This study
pSM5	Complete *opd* gene encoding preOPH, cloned in pMMB206 as EcoRI and HindIII fragment, Cm^{r}	13
pSDP5	*orf306* cloned as a NcoI-BamHI fragment in pET15b, Codes for native Orf306, Amp^{r}	This Study
pNS1	4. 5 kb *hca* operon cloned in pET23b as NdeI / SalI fragment. Expresses $HcaEFBCD^{6His}$. Only HcaD contains C-terminal His tag.	This work
pGS1	*hcaR-lacZ* fusion generated by cloning *hcaR* promoter as E. coRI/PstI fragment in pMP220.	This work
pSDP14	*mhpA-lacZ* fusion generated by cloning *mhpA* promoter as E. coRI/PstI fragment in pMP220	This work

pSDP15	*mhpR-lacZ* fusion generated by cloning mhpR promoter as E. coRI/PstI fragment in pMP220	This work

TABLE 2

Primer name	Sequence (5'- 3')	Purpose
SDP13 F SDP14 R	ATCTTTCAGGATTAAAAAAT CTCTAGTGAAACTTGCGCAC	*hca*E-knockout
SDP15 F SDP16 R	GAACCGAGTCGTGAGGTACT AGTGAAGATAAGCGTGCATA	*mhp*A-knockout
SDP17 F SDP18 R	ATTTTGTTGTTAAAAACATGTAA CCACCAGAATAGCCTGCGAT	*mhp*R-knockout
SDP19 F SDP20 R	GCTATCGAGCCACAGGACTG ATTACTCATTTTGAATCTCC	*paa*A-knockout
SDP21 F SDP22 R	AACATCTGACGAGGTTAATA CGTTTTTTTGTCTGAAACAA	*mao*A-knockout
SDP31 F SDP32 R	AGTCGAACGGTAACAGGAAGA GCAATATTCCCCACTGCTG	*16s rRNA-qPCR*
SDP33 F SDP34 R	GAAAGAGCACGATCGCGTGG TTGCTCGGAATAAACGCCGC	*aceB-qPCR*
SDP35 F SDP36 R	GAAAGAGCACGATCGCGTGG GCAAGCTGGCGAATAGCGTT	*aceK-qPCR*
SDP37 F SDP38 R	TAAGGACACGTTGCAGGCCA GGCGGTAGGCAATTTCACGG	*acnA-qPCR*
SDP39 F SDP40 R	TGGTTCCCGTGAAGCTCTGG TGCAGCAGCTTTGGCGTTAG	*eno-qPCR*
SDP41 F SDP42 R	CAATTCGCGGGGTTGTTCGT GGTTTTCGATAGCCACGGCG	*pfkA-qPCR*
SDP43 F SDP44 R	GCAGAAATGCTGGCGCGTAT ATGTGCCCGCCGTTACCATA	*fad*A-*qPCR*
SDP45 F SDP46 R	ACCGCTAATGAAGTGGCCGA CTGCACAACGCCGACAGTTT	*fad*R-*qPCR*
SDP47 F SDP48 R	TGCTCGGTATGGCACCGAAT GGCTTTGATCCAAGGCGTCG	*glc*B-*qPCR*
SDP49 F SDP50 R	TACTGAAGGTCGGTCAGCCG CCTCCAGTAATGCGCGAACG	*glc*C-*qPCR*
SDP51 F SDP52 R	CGAAGGCGGCACCGAAATTG CGGGCGGTTTGTCCATCACC	*hca*E-*qPCR*
SDP53 F SDP54 R	CAGACAGCCAGACACCTTGA CGGATCGGTACTGACGAAA	*hca*R-*qPCR*
SDP55 F SDP56 R	CCCGGTTGGGCTGATGATGG CGGCGTAGTGTGCGGCAGAA	*mhp*A-*qPCR*
SDP57 F SDP58 R	GCGGTACGGCGATAGAGGCG ACCTGGCTGGCCTTTTGCCC	*mhp*R-*qPCR*
SDP59 F SDP60 R	CCACCGACGAATTACGCAGC TTCACCTGGCTACGGGCAAA	*prp*B-*qPCR*
SDP61 F SDP62 R	TATTTTGCCCGCCACGATGC GCGGCATTTCGCCAATCTCA	*prp*R-*qPCR*

Orf306F2 Orf306R3	GGCTGCCATCATCCCATGGGAACACCCGCTA CGCGGATCCCTATTCCCCGTCAAGATAC	Amplification of *orf306* as NcoI- BamHI fragment to be cloned in pET15b
Orf306F5	GGCTGCCATCATCGGATCCGAACACCCGCTA	Amplification of *orf306* as a BamHI fragment using Orf306R3 as reverse primer to be cloned in pGEX4T1
HcaRFP1 HcaRRP1	AGGAATTCAAGCTCCAGTTGGTAA ACCTGCAGACGGGTAAAGTTCAGT	Amplification of hcaR promoter to be cloned in pMP220
HcapET23bFP1 HcapET23bRP1	ATACGCATATGACCACACCCTCAGATTTGAA ACTACGTCGACCAGTGATTTAAGCGCGATGTT	Amplification of *hca* operon as a NdeI- SalI fragment using pET23b
MhpRF MhpRR	CCGAGCTGCAGATTAATTGACATTTCTATA CCGGAGAATTCTTCAGTACCTCACGAC	Amplification of *mhpR* promoter to be cloned in pMP220

FIGURE 1

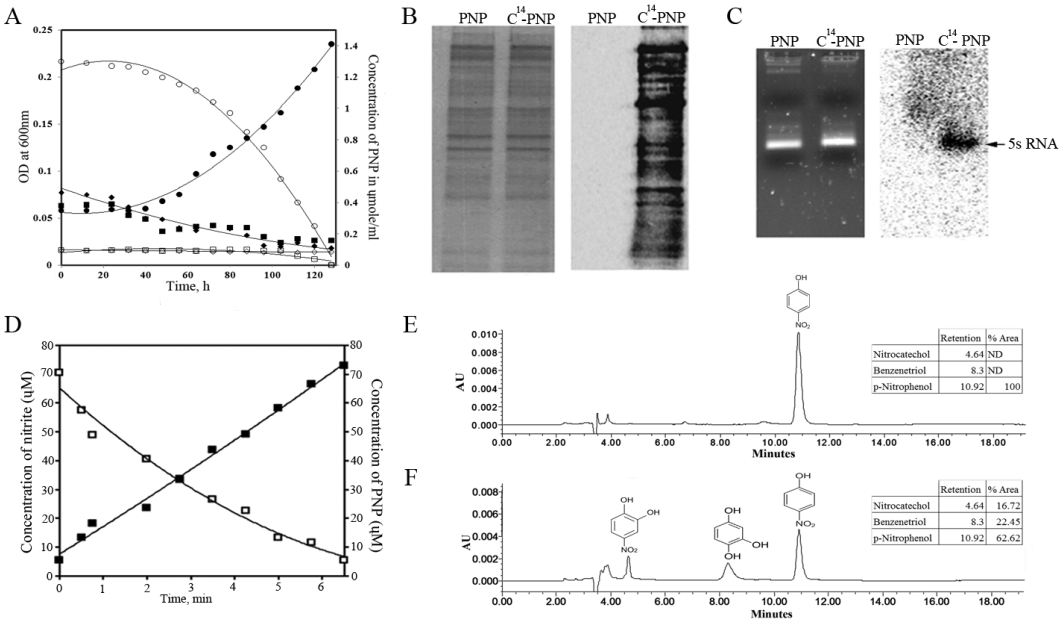

FIGURE 2

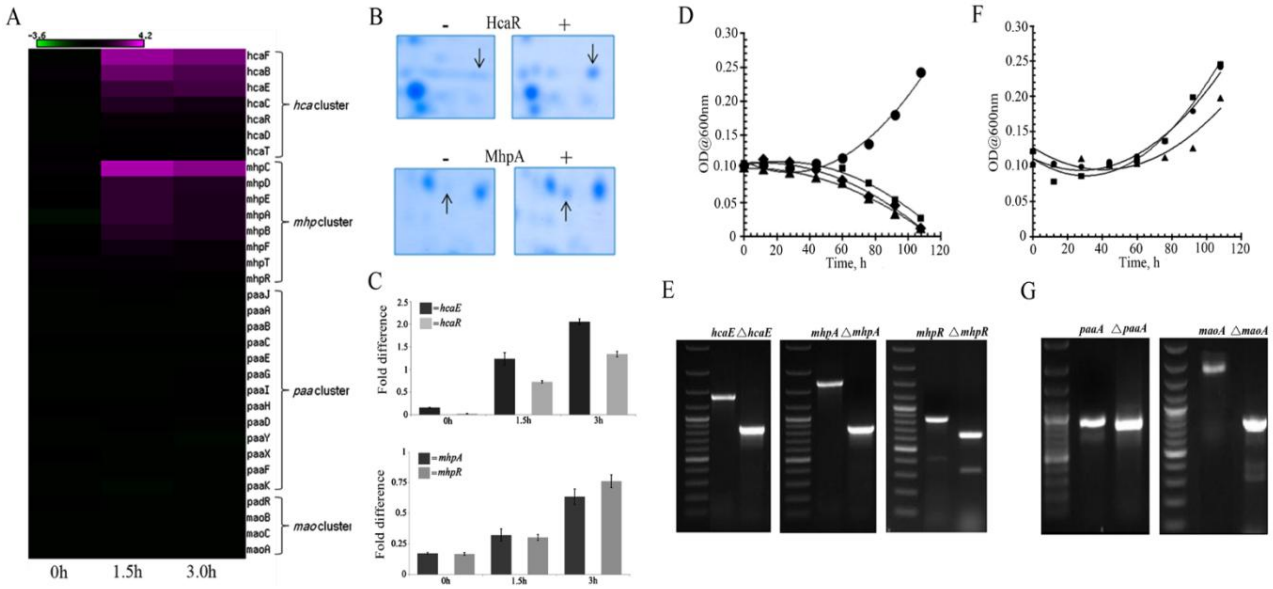

FIGURE 3

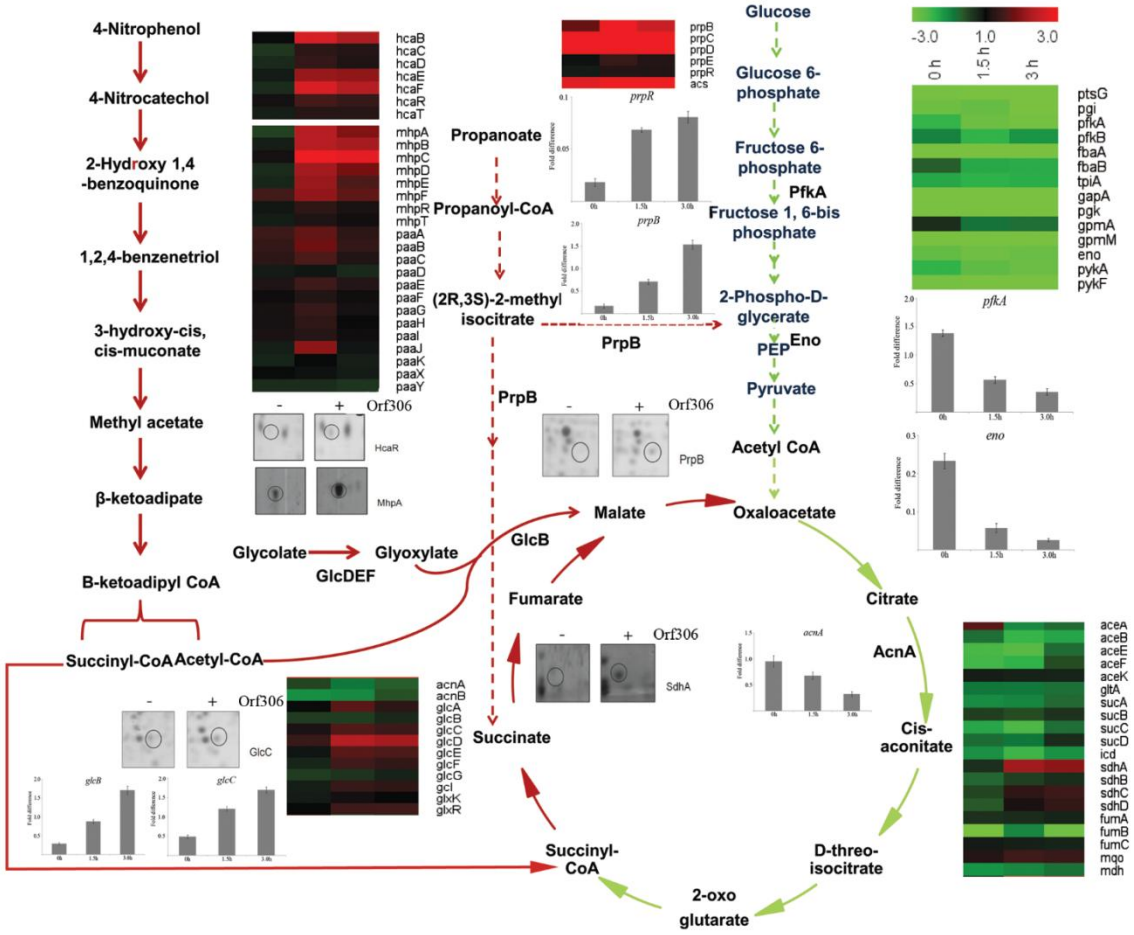

FIGURE 4

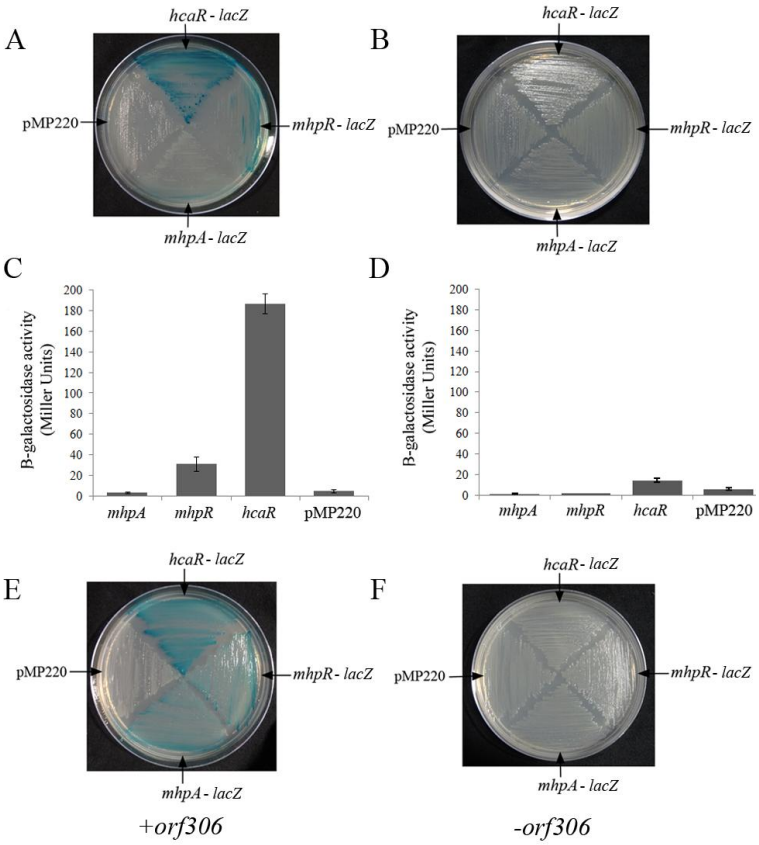

FIGURE 5

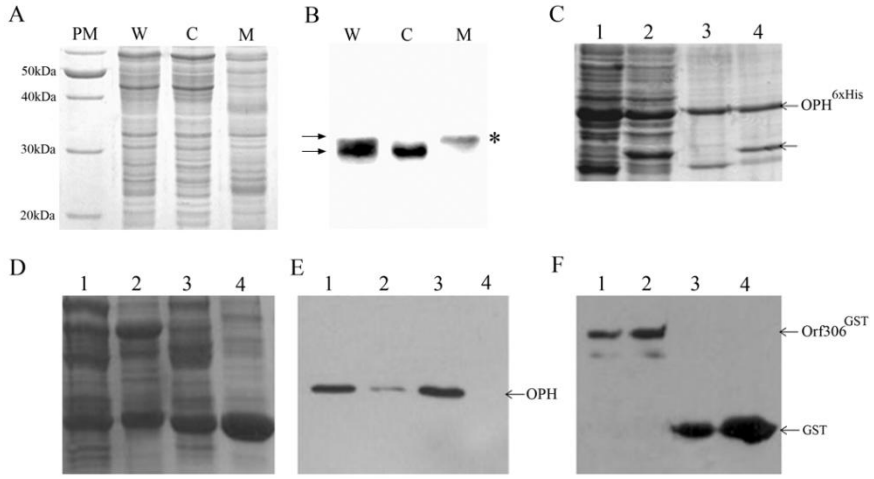

The organophosphate degradation (opd) island borne esterase induced metabolic diversion in E. coli and its influence on p-nitrophenol degradation

Deviprasanna Chakka, Ramurthy Gudla, Ashok Kumar Madikonda, Emmanuel Vijay Paul Pandeeti, Sunil Parthasarathy, Aparna Nandavaram and Dayananda Siddavattam

J. Biol. Chem. published online October 9, 2015